Model of line-of-sight ultraviolet propagation

BIFENG LI[1*], HONGXING WANG[1], ZHONGYANG MAO[1], ZHENLONG DONG[1], XIONG ZHANG[2]

[1]Department of Electronic and Information Engineering, Navy Aeronautical Engineering University,
  Yantai, Shangdong 264001, China

[2]Unit 92198, Xingcheng, Liaoning 125109, China

*Corresponding author: lbfandwy@163.com

The traditional line-of-sight ultraviolet model cannot serve better for link performance study for the reason that the scattering characteristic is often ignored in the modelling process. Therefore, a line-of-sight ultraviolet bipyramid model in combination with transceiver full beam angles and geometrical relationship of the transceiver field of view intersection is established. The theoretical rationality of the bipyramid model in comparison with a traditional line-of-sight model is demonstrated by the classically analytical model for line-of-sight scenario. Based on a bit error rate requirement of voice communication, the effects of transmitting power *versus* range for three line-of-sight ultraviolet communication modes are further analyzed.

Keywords: ultraviolet communication, bipyramid model, scattering characteristic, line-of-sight (LOS) communication mode.

1. Introduction

Due to the absorption of ozone in the stratosphere, the solar ultraviolet radiation of 200–300 nm forms a solar blind region not varying with season near the ground. As ultraviolet (UV) communication works at the above wavelength band, it can maximally reduce the background noise and correspondingly realize wide-field receiving. Additionally, signals beyond the extinction range can hardly be intercepted due to the strong absorption and scattering of molecules and aerosol particles in the atmosphere, and the APT (acquisition, pointing, tracking) requirement is relieved because of scattering characteristic. Consequently, UV communication has been one of the research hotspots of wireless optical communication in recent years.

Non-line-of-sight (NLOS) UV communication usually attracts people's attention for the reason of its scattering characteristic. Based on the prolate-spheroidal coordinate system, a widely adopted yet complex single scattering channel model was built

for coplanar scenario in [1]. For noncoplanar geometry, the generalized models with the consideration of transceiver cone axes pointing in arbitrary directions were proposed and developed in [2, 3]. Nevertheless, for the purpose of tractable analysis, the approximate models without an integral form were studied in [4–6] for the assumption that the transceiver beam angles are small. In contrast, line-of-sight (LOS) communication, which is recognized as a typical form of NLOS communication and defined as a scenario of transceiver beam axes coinciding at the basic axis with opposite direction, is often ignored. However, there are some potential military scenes for LOS UV communication, such as the warship formation sailing out and the communication between the coast and island with no obstacles in the link, for which LOS communication can perform better in actual environment. In the existing literature of LOS UV modelling, a model combined with free space path loss was established on the grounds of free space optical (FSO) modelling theory in [7]. Nevertheless, the model ignored the influence of transceiver beam angles on LOS link, and was not distinguished from traditional FSO channel model by scattering characteristic.

   To establish a reasonable LOS UV model for link performance study and system design, this paper is organized as follows. First, the geometrical link and bipyramid model for LOS UV communication are studied in Section 2. Then, the bit error rate (BER) performance on the basis of the established model for LOS link is described in Section 3. The numerical simulation of path loss and link performance in terms of transceiver beam angles are given in Section 4. Finally, some conclusions are drawn in Section 5.

2. LOS UV channel model

More attention is paid to the atmospheric transmission of light propagation in FSO, and the factors of transceiver beam angles are embodied in the geometrical attenuation. However, it can adopt wide-field receiving for LOS UV communication due to the scattering characteristic, correspondingly, the influence of transceiver beam angles should be considered while modelling. According to different transceiver beam angles, LOS UV communication can be divided into three modes, which are defined as narrow beam angle transmitting to narrow field of view (FOV) receiving (Fig. 1**a**), narrow beam angle transmitting to wide FOV receiving (Fig. 1**b**) and wide beam angle transmitting to wide FOV receiving (Fig. 1**c**). Note that the transmitting beam angle is less
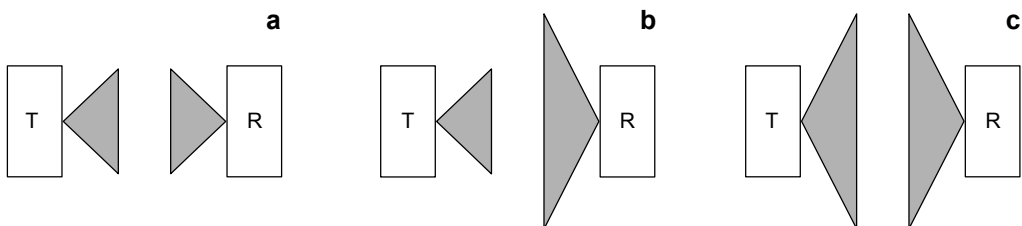

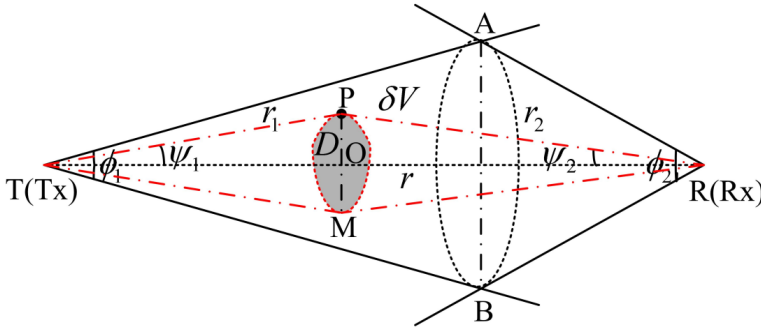Fig. 1. LOS UV communication modes (see text for explanation).

Fig. 2. Geometrical link of LOS UV communication based on single-scattering assumption (see text for explanation).

than the receiving FOV for the reasons of reducing energy loss and maximizing receiving energy.

Figure 2 depicts a geometrical link of LOS UV communication based on single-scattering assumption, the transmitter (Tx) and receiver (Rx) are located at points T and R. A and B depict the upper and bottom intersections of transceiver FOV, respectively. We define the basic parameters as follows, let ϕ_1 and ϕ_2 be the Tx full beam angle and Rx FOV, r the Tx and Rx baseline separation. As we can know from the scattering characteristic of UV communication, the scattering occurs in the intersection of transceiver FOV. It is not difficult to find out that the effective scattering volume is a bipyramid for LOS communication, as the enclosed volume V_{ATBR} shown in Fig. 2. For any point P and its symmetric point M around the basic axis in the bipyramid, let us denote PT and PR as the r_1 and r_2 which are distances of the common volume to the Tx and Rx, and the angles between PT and TR, PR and TR as the ψ_1 and ψ_2, respectively. PM is perpendicular to TR with an intersection O. Similar to the process of NLOS UV scattering communication, we primarily consider single-scatter propagation and regard the whole communication link as two stages, from the effective scattering volume to the Tx and Rx, respectively.

Assume the power P_t of UV LED source is transmitted uniformly over the Tx solid cone angle Ω_t into a homogeneous and isotropic medium and the point P, which is apart from the Tx with r_1. If P lies inside the Tx cone, the power per unit area at P is [1]

$$H_P = \frac{P_t \exp(-k_e r_1)}{\Omega_t r_1^2} \tag{1}$$

where $\Omega_t = 2\pi[1 - \cos(\phi_1/2)]$, is the atmospheric extinction coefficient obtained from the absorption coefficient k_a and scattering coefficient k_s by $k_e = k_a + k_s$. A differential volume δV enclosing P can now be regarded as a secondary source with power

$$\delta Q_P = k_s H_P \delta V = \frac{k_s P_t \exp(-k_e r_1)}{\Omega_t r_1^2} \delta V \tag{2}$$

Then the power transmitted per unit solid angle from this secondary source is a function of the scattering angle θ_s

$$\delta R_P = \delta Q_P P(u) \tag{3}$$

where the scattering phase function $P(u)$ is modeled as a weighted sum of the Rayleigh (molecular) and Mie (aerosol) scattering phase functions based on the corresponding scattering coefficients [8]

$$P(u) = \frac{k_s^{\text{Ray}}}{k_s} p^{\text{Ray}}(u) + \frac{k_s^{\text{Mie}}}{k_s} p^{\text{Mie}}(u) \tag{4}$$

where $u = \cos(\theta_s)$, θ_s is zero for LOS UV communication, $k_s = k_s^{\text{Ray}} + k_s^{\text{Mie}}$. The Rayleigh and Mie scattering phase functions follow a generalized Rayleigh model [9] and a generalized Henyey–Greenstein function [10], respectively,

$$p^{\text{Ray}}(u) = \frac{3\left[1 + 3\gamma + (1 - \gamma)u^2\right]}{16\pi(1 + 2\gamma)} \tag{5}$$

$$p^{\text{Mie}}(u) = \frac{1 - g^2}{4\pi}\left[\frac{1}{(1 + g^2 - 2gu)^{3/2}} + \frac{f(3u^2 - 1)}{2(1 + g^2)^{3/2}}\right] \tag{6}$$

where γ, g and f are model parameters.

The power per unit area at the Rx that is due to the differential volume source is

$$\delta P_r = \frac{\delta R_P \cos(\zeta) \exp(-k_e r_2)}{r_2^2} = \frac{P_t P(u) \cos(\zeta) \exp\left[-k_e(r_1 + r_2)\right]}{\Omega_t (r_1 r_2)^2} \delta V \tag{7}$$

where ζ is the angle between the Rx axis and a vector from the Rx to the common volume, and equal to ψ_2 as shown in Fig. 2. If we define the differential volume δV as a hollow bipyramid, it is easy to observe that all the points on its intersecting part described as a circle have the same propagation path. According to Fig. 2, the geometrical relationship between r_1, r_2 and r, ψ_1, ψ_2 can be given by

$$\begin{cases} r_1 \cos(\psi_1) + r_2 \cos(\psi_2) = r \\ r_1 \sin(\psi_1) = r_2 \sin(\psi_2) = PO \end{cases} \tag{8}$$

Solving Eq. (8), results in the following expression

$$\begin{cases} r_1 = \dfrac{r \sin(\psi_2)}{\sin(\psi_1 + \psi_2)} \\ r_2 = \dfrac{r \sin(\psi_1)}{\sin(\psi_1 + \psi_2)} \end{cases} \tag{9}$$

Denote *PO* as *x*, the differential volume δV can be expressed as

$$\delta V = \frac{2\pi x \mathrm{d}x \left[r_1 \cos(\psi_1) + r_2 \cos(\psi_2) \right]}{3} = \frac{2\pi r^2 \sin(\psi_1) \sin(\psi_2)}{3 \sin(\psi_1 + \psi_2)} \mathrm{d}x \tag{10}$$

where the differential length $\mathrm{d}x$ is deduced as follows

$$\mathrm{d}x = \frac{\partial x}{\partial \psi_1} \mathrm{d}\psi_1 + \frac{\partial x}{\partial \psi_2} \mathrm{d}\psi_2 =$$

$$= \left[\frac{\sin^2(\psi_2)}{\sin^2(\psi_1 + \psi_2)} \mathrm{d}\psi_1 + \frac{\sin^2(\psi_1)}{\sin^2(\psi_1 + \psi_2)} \mathrm{d}\psi_2 \right] r \tag{11}$$

Substituting Eqs. (9)–(11) into (7), leads to the total receiving power

$$P_r = \frac{P_t P(u) k_s A_r}{3r[1 - \cos(\phi_1/2)]} \int_l (A \mathrm{d}\psi_1 + B \mathrm{d}\psi_2) =$$

$$= \frac{P_t P(u) k_s A_r}{3r[1 - \cos(\phi_1/2)]} \iint_D \left(\frac{\partial B}{\partial \psi_1} - \frac{\partial A}{\partial \psi_2} \right) \mathrm{d}\psi_1 \mathrm{d}\psi_2 \tag{12}$$

where

$$A = \exp\left[-k_e r \frac{\sin(\psi_1) + \sin(\psi_2)}{\sin(\psi_1 + \psi_2)} \right] \frac{\sin(\psi_2) \cos(\psi_2) \sin(\psi_1 + \psi_2)}{\sin(\psi_1)} \tag{13a}$$

$$B = \exp\left[-k_e r \frac{\sin(\psi_1) + \sin(\psi_2)}{\sin(\psi_1 + \psi_2)} \right] \frac{\sin(\psi_1) \cos(\psi_2) \sin(\psi_1 + \psi_2)}{\sin(\psi_2)} \tag{13b}$$

$$\frac{\partial B}{\partial \psi_1} - \frac{\partial A}{\partial \psi_2} = \exp\left[-k_e r \frac{\sin(\psi_1) + \sin(\psi_2)}{\sin(\psi_1 + \psi_2)} \right] \times$$

$$\times \left[-\frac{2\sin(\psi_1 - \psi_2) + 3\sin(2\psi_2)\cos(\psi_1 + \psi_2)}{2\sin(\psi_1)} + \frac{\cos(\psi_2)\sin(2\psi_1 + \psi_2)}{\sin(\psi_2)} + \right.$$

$$\left. + k_e r \frac{\cos(\psi_2)\left[\sin(\psi_2) - \sin(\psi_1) \right]\left[1 - \cos(\psi_1 + \psi_2) \right]}{\sin(\psi_1 + \psi_2)} \right] \tag{13c}$$

The integral subscript *l* of Eq. (12) is a vector curve defined as the intersecting circle of hollow bipyramid with anticlockwise direction, correspondingly, the enclosed area *D* described as the shadow in Fig. 2 is determined by ψ_1 and ψ_2 with the definition

$D = \{(\psi_1, \psi_2)|0 \le \psi_1 \le \phi_1/2, 0 \le \psi_2 \le \phi_2/2\}$; A_r is the effective area of the Rx. If we define the path loss as $L = P_t/P_r$, the path loss for LOS UV communication link is then obtained by

$$L = \frac{3r\left[1 - \cos(\phi_1/2)\right]}{P(u)k_s A_r} \left[\iint_D \left(\frac{\partial B}{\partial \psi_1} - \frac{\partial A}{\partial \psi_2}\right) d\psi_1 d\psi_2\right]^{-1} \tag{14}$$

3. Link performance

Assume the bandwidth of the detector is limited to twice of the data rate, for direct detection, the quantum-limit based receive signal noise ratio (SNR) becomes [11]

$$SNR = \frac{\eta_r G P_r}{2Rhc/\lambda} \tag{15}$$

where G is the photomultiplication gain of the detector, typically G equals 30–50 for avalanche photodiode (APD), and 10^3–10^5 for photomultiplier tube (PMT); η_r is the detector quantum efficiency, R is the data rate, h is the Planck constant, and c is the light speed. Substituting Equation (12) into Eq. (15), leads to the following SNR expression

$$SNR = \frac{G P_t P(u)k_s \eta_r \lambda A_r}{6Rhcr\left[1 - \cos(\phi_1/2)\right]} \iint_D \left(\frac{\partial B}{\partial \psi_1} - \frac{\partial A}{\partial \psi_2}\right) d\psi_1 d\psi_2 \tag{16}$$

The BER for detection of on-off keying signals is given by [11, 12]

$$BER = Q\left(\frac{\sqrt{SNR}}{2}\right) = \frac{1}{2}\,\text{erfc}\left(\frac{\sqrt{SNR}}{2\sqrt{2}}\right) \tag{17}$$

where $Q(...)$ and erfc(...) are Q-function and complementary error function, respectively.

4. Simulation study

To further study the influences of transceiver beam angles on LOS UV communication link, let us select typical figures of parameters during the numerical simulation. Assume there is no turbulence. The parameters are set as follows, $\gamma = 0.017$ [9], $g = 0.72$ and $f = 0.5$ [10], $(k_a, k_s^{\text{Ray}}, k_s^{\text{Mie}}) = (0.9, 0.24, 0.25)$ km^{-1} at $\lambda = 260$ nm [13], a LED array with $P_t = 50$ mW, $\eta_r = 0.2$, $A_r = 1.77$ cm^2 [8], $G = 100$. In comparison with analytical model for LOS scenario [1] and traditional LOS UV model [7], Fig. 3 shows the path loss *versus* Tx beam angle for 1 km link distance. Good agreement between the bipyramid model and the analytical model is observed, which indicates the rationality of bipyramid model. However, there are great differences about 9–20 dB between
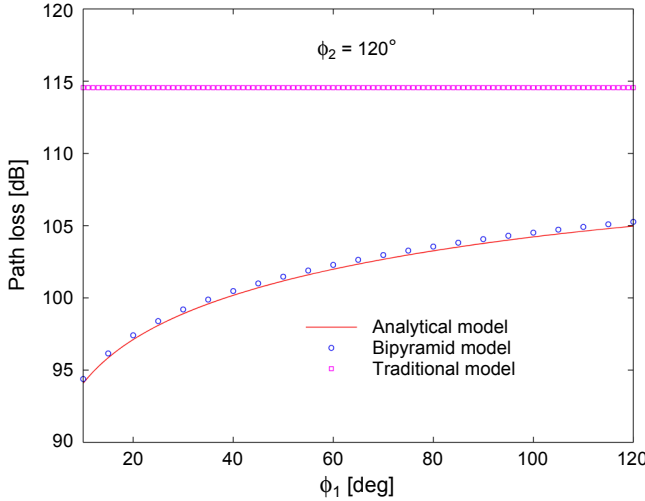
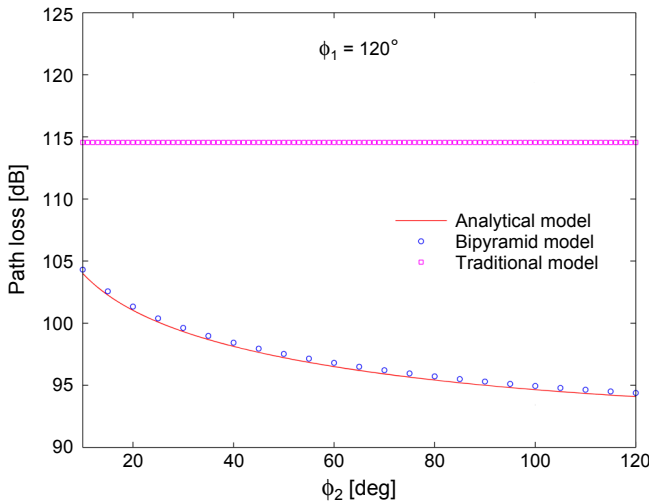Fig. 3. Path loss *versus* Tx beam angle for 1 km link distance.

Fig. 4. Path loss *versus* Rx FOV for 1 km link distance.

the traditional model and the analytical model. It is not hard to find that the path loss increases nonlinearly with Tx beam angle until there is a saturation point at about $\phi_1 = 100°$. Similarly, the influences of Rx FOV on model agreement can also be observed in Fig. 4. Nevertheless, 10–20 dB differences occur between the traditional model and the analytical model, meanwhile, the path loss decreases nonlinearly with Rx FOV until the saturation point at about $\phi_2 = 100°$.

As we can know from the simulation analysis of Figs. 3 and 4, transceiver beam angles have great influence on LOS UV communication link and cannot be ignored. The applicability of traditional LOS UV model based on FSO modelling theory yet

without considering the effects of transceiver beam angles is restricted. The influence of transceiver beam angles on path loss is consistent with actual situation. This is because the great energy loss occurs due to enlarging the extinguished probability of photon scattering as increasing the Tx beam angle. On the contrary, more receiving energy is obtained for the reason of raising the probability that the photon arrives at Rx within its FOV after scattering when increasing the Rx FOV. Consequently, the established LOS UV model based on scattering characteristic has the theoretical rationality for system design and performance analysis.
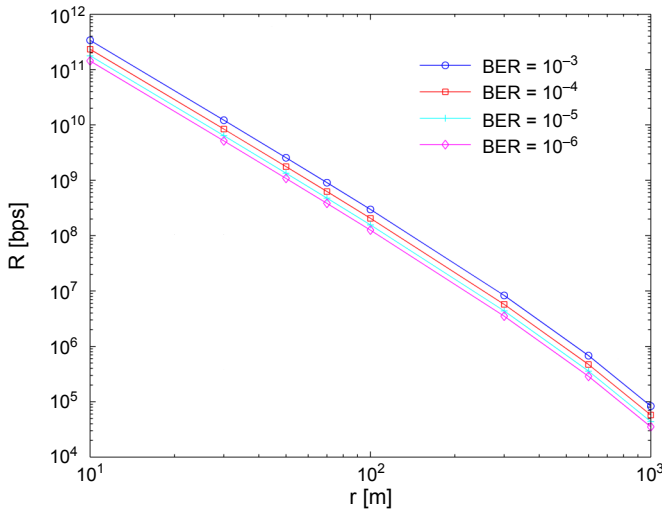

Fig. 5. Data rate *versus* range for different BER.

According to Eqs. (16) and (17), it is an interesting work to study the LOS UV link performance for the trade-off relationship among the range, rate, transmitting power, path loss and BER. Following the former parameters settings except for $(\phi_1, \phi_2) = (30°, 60°)$, Fig. 5 depicts data rate *versus* range, with curves parameterized by the BER. The data rate decreases linearly with range, and slowly as raising one level of BER requirements for BER $\geq 10^{-4}$. For BER requirements of 10^{-3} (voice service) and 10^{-6} (data service), data rate can achieve 300 Mbps and 125 Mbps for 100 m range, 80 kbps and 35 kbps for 1 km range, respectively. For LOS UV voice communication system, Fig. 6 shows transmitting power *versus* range with BER of 10^{-3} and data rate of 20 kbps for three LOS communication modes, which are narrow beam angle transmitting to narrow FOV receiving with $(\phi_1, \phi_2) = (10°, 10°)$, narrow beam angle transmitting to wide FOV receiving with $(\phi_1, \phi_2) = (10°, 120°)$ and wide beam angle transmitting to wide FOV receiving with $(\phi_1, \phi_2) = (120°, 120°)$, and are represented by *A*, *B* and *C*, respectively. Fix the range, there are great differences among the transmitting power requirements of the three modes, where the transmitting power require-
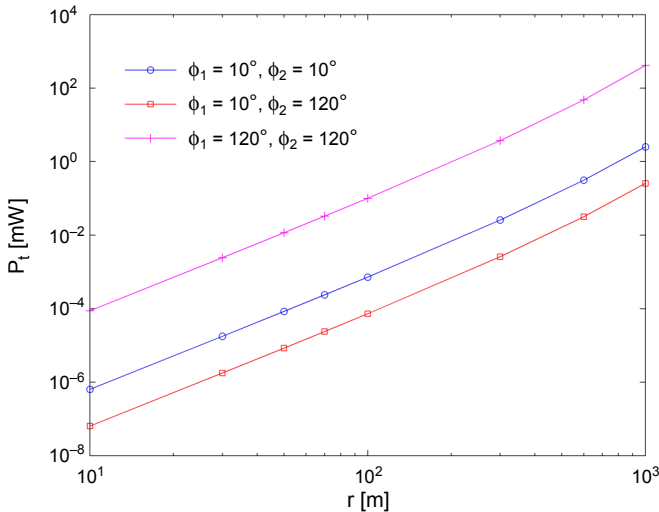
Fig. 6. Transmitting power *versus* range for three LOS communication modes.

ment of *A* takes the first place, then followed by *C*, and *B* is the smallest one. Consequently, the *B* mode, whose power requirement is less than 1 mW for 1 km range, is most favorable for LOS UV communication.

5. Conclusions

Based on the influences of transceiver beam angles on UV scattering propagation, a LOS UV bipyramid model is established. In comparison with traditional LOS UV model, the theoretical rationality of bipyramid model is demonstrated by a classically analytical model for LOS scenario. Besides, for a BER requirement of voice communication, the effects of transmitting power *versus* range for three LOS UV communication modes are analyzed, and the narrow beam angle transmitting to wide FOV receiving shows the best effect. In the future, we will use the UV communication system constructed by a special communication laboratory to improve the established LOS model in field experiments.

References

[1] LEUTTGEN M.R., REILLY D.M., SHAPIRO J.H., *Non-line-of-sight single-scatter propagation model*, Journal of the Optical Society of America A **8**(12), 1991, pp. 1964–1972.
[2] HOUFEI XIAO, YONG ZUO, JIAN WU, HONGXIANG GUO, JINTONG LIN, *Non-line-of-sight ultraviolet single-scatter propagation model*, Optics Express **19**(18), 2011, pp. 17864–17875.

[3] YONG ZUO, HOUFEI XIAO, JIAN WU, YAN LI, JINTONG LIN, *A single-scatter path loss model for non-line-of-sight ultraviolet channels*, Optics Express **20**(9), 2012, pp. 10359–10369.

[4] SUNSTEIN D.E., *A Scatter Communications Link at Ultraviolet Frequencies*, Thesis, Massachusetts Institute of Technology, Department of Electrical Engineering, 1968.

[5] LEIJIE WANG, ZHENGYUAN XU, SADLER B.M., *An approximate closed-form link loss model for non-line-of-sight ultraviolet communication in noncoplanar geometry*, Optics Letters **36**(7), 2011, pp. 1224–1226.

[6] KE XIZHENG, *Theory of Ultraviolet Self-Organizing Network*, 1st Ed., Science Press, Beijing, 2011, pp. 63–66.

[7] ZHENGYUAN XU, *Approximate performance analysis of wireless ultraviolet links*, IEEE International Conference on Acoustics, Speech and Signal Processing, ICASSP 2007, Vol. 3, pp. III-577–III-580.

[8] ZHENGYUAN XU, HAIPENG DING, SADLER B.M., GANG CHEN, *Analytical performance study of solar blind non-line-of-sight ultraviolet short-range communication links*, Optics Letters **33**(16), 2008, pp. 1860–1862.

[9] BUCHOLTZ A., *Rayleigh-scattering calculations for the terrestrial atmosphere*, Applied Optics **34**(15), 1995, pp. 2765–2773.

[10] ZACHOR A.S., *Aureole radiance field about a source in a scattering–absorbing medium*, Applied Optics **17**(12), 1978, pp. 1911–1922.

[11] GAGLIARDI R.M., KARP S., *Optical Communication*, 2nd Ed., John Wiley & Sons, New York, 1995, Chap. 2.

[12] ANDREWS L., PHILLIPS R.L., *Laser Beam Propagation through Random Media*, 2nd Ed., SPIE Press, Bellingham, Washington, 2005, pp. 445–447.

[13] SHAW G.A., NISCHAN M.L., IYENGAR M.A., KAUSHIK S., GRIFFIN M.K., *NLOS UV communication for distributed sensor systems*, Proceedings of SPIE **4126**, 2000, pp. 83–96.